GEOPHYSICAL RESEARCH LETTERS, VOL. 28, NO. 9, PAGES 1903-1906, MAY 1, 2001

Mesospheric planetary waves at northern hemisphere fall equinox

H.-L. Liu, R. G. Roble

NCAR High Altitude Observatory, Boulder, Colorado

M. J. Taylor, W. R. Pendleton, Jr.

Space Dynamics Laboratory & Department of Physics, Utah State University, Logan, Utah

Abstract.
Northern hemisphere planetary waves are strong in the winter and weak in the summer, and they go through a fast transition around equinox. This transition is studied here using NCAR Thermosphere-Ionosphere-Mesosphere-Electrodynamics general circulation model (TIME-GCM) simulations with 1997 National Centers for Environmental Prediction (NCEP) analysis. The planetary wave variability during the transition and its effect on the temperature and winds in the mesosphere are examined. The simulated planetary wave structure agrees with climatological studies, and the fast transition of the planetary waves is captured by the model. The wave variability produces large temperature changes in the upper atmosphere above local stations in middle and high latitudes. The qualitative behavior of the model is in excellent agreement with recent observations of a major perturbation in OH mesospheric temperatures from Ft. Collins (Taylor et al., 2001), although the smaller calculated magnitude suggests that the planetary wave amplitude might be underestimated by the model.

1. Introduction

The propagation and growth of planetary waves are strongly dependent on the background atmospheric wind system. Theoretical studies show that the westerly wind in the middle atmosphere during winter is favorable for the propagation of the small wave number planetary waves (cf. Charney and Drazin, 1961). This is supported by climatological studies from both ground based and satellite measurements. Barnett and Labitzke (1990) show that the planetary wave perturbations of geopotential height and temperature are strongest during the winter season between ~20 km and ~80 km. Wind measurements from the Upper Atmospheric Research Satellite(UARS) High Resolution Doppler Imager (HRDI) suggest strong planetary wave activity as well as large variations due to interactions with gravity waves during winter (Smith, 1996). More recently, Wang et al. (2000) inferred planetary wave structures in horizontal wind in the lower thermosphere from the UARS Wind Imaging Interferometer (WINDII), and it is found that the stationary planetary wave 1 is strong at solstice and wave 2 is strong around equinox. Because the extratropical strato-mesospheric zonal mean wind changes direction around equinox, it is a transitional period for the planetary wave propagation between the summer characteristics (weak planetary wave) and winter characteristics (strong planetary wave). The climatological studies by Barnett and Labitzke (1990) indeed show that the planetary waves (especially wave 1) change significantly around both spring and fall equinoxes. Furthermore, the in situ forcing of planetary waves should also change as a result of changes in the mean winds as well as wind filtering of gravity waves. The equinox transition may produce large wave transience and variability in wind, temperature, and hence airglow emissions. Large variations of the OI 557.7nm airglow emissions at middle and high latitudes are observed around the spring equinox by ground based instrumentation and WINDII (Shepherd et al., 1999). More recently, an exceptionally large amplitude perturbation in mesospheric temperature was observed around the fall equinox from Ft. Collins (41°N, 105°W) by Taylor et al. (2001). They also found that a large departure from the nominal seasonal temperature (~25-30 K) occurs over an interval of approximately 3-4 weeks shortly after the fall equinox.

In this study, the fall equinox period for 1997 is simulated by the NCAR TIME-GCM with 1997 NCEP forcing at the lower boundary of the model (~10 mb). The model simulations predict transition of the planetary waves consistent with the climatology and temperature variations qualitatively similar to the aforementioned observations.

2. Numerical Model

The TIME-GCM (Roble and Ridley, 1994) is a three-dimensional general circulation model that includes the relevant physics and chemistry to self-consistently predict the response of the neutral atmosphere to tides and other atmospheric waves from 30 to 500 km. The model

Paper number 2000GL012689.
0094-8276/01/2000GL012689$05.00

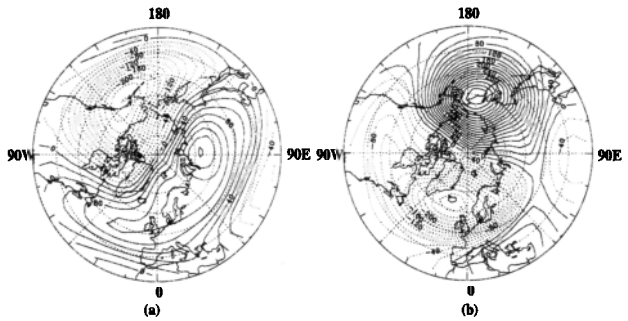

Figure 1. Geopotential height perturbations on day (a)260 and (b) 280 at 10 mb (NCEP 1997) from 30°N to north pole. Solid contours are positive values and contour interval is 20 m

setup is similar to that described in Waltercheid et al. (2000), except that the daily variation of geopotential and temperature according to NCEP analysis (Randel, 1992) is specified at the lower boundary for the period July 1-October 31 of 1997 for the run used in this paper.

3. Results and Analysis

Analysis of the NCEP geopotential height at 10 mb indicates significant variations in the planetary waves from day 260 to day 290, with the general trend of a growing planetary wave 1 component. Figure 1 shows the geopotential height perturbation on day 260 and 280. The wave 1 component on day 280 has increased significantly and becomes the dominant feature. The phase of the wave 1 component also changes during the same period of time. Zonal wavenumber-frequency analysis (not shown) shows that the planetary wave 1 has an average amplitude of ~100 m between day 260 and 273 and then increases to a peak value of ~270 m on day 280. It decreases slightly and stays above 200 m between day 280 and day 290. The phase shifts by about 120° eastward between day 260 and 280.

The increased planetary wave activity evident in the lower stratospheric forcing penetrates into the mesosphere. This is demonstrated in Figure 2, which shows the Eliassen-Palm (EP) flux on days 260 and 285. The EP flux on day 285 increases at almost all altitudes in the middle/high latitude stratospheric and mesospheric region, with preferred upward/equatorward propagation. It is evident from Figure 2 that the planetary wave propagation and growth are sensitively dependent on the zonal wind, because the maximum westerly wind corresponds roughly to the minimum refractive index for planetary waves. Therefore, planetary waves refract away from the region of maximum westerly winds as shown in Figure 2. In addition, divergence of the EP flux shows that the planetary wave produces westward forcing above 80 km at middle/high latitudes with a peak value of ~30 $ms^{-1}day^{-1}$ at 70°N on day 285, compared with almost zero forcing on day 260. Therefore, planetary wave forcing appears to complement gravity wave forcing in driving the wind reversal in the mesosphere and lower thermosphere around the fall equinox.

The planetary wave 1 growth around fall equinox can also be seen from the temperature perturbations. Figure 3(a) and (b) show longitude-latitude cross section of the planetary wave 1 component of the temperature perturbation at about 87 km on days 260 and 285. On day 260, the dominant source of the planetary wave 1 is in the southern hemisphere, and its amplitude at middle/high latitudes in the northern hemisphere is less than 1 K. The planetary wave 1 amplitude in the northern hemisphere is much larger on day 285 with a peak value of 12 K between 60°N and 70°N with phase lines tilting westward with decreasing latitudes (and increasing altitudes, not shown). These agree with the climatological features of the planetary wave under winter conditions (Barnett and Labitzke, 1990). Therefore, the model reproduces the rapid transition of planetary wave 1 from summer characteristics to winter characteristics around the fall equinox within less than a month. This fast transition is consistent with the September and October climatological results (Barnett and Labitzke, 1990). Figure 3(c) and (d) are the temperature changes at the same altitude as a function of time above two locations: 105°W and 70°E and both at 42.5°N. They show a superposition of variations due to tidal waves and planetary waves. The crosses indicate temperature values at local night (2000LT-0400LT) as measured by ground based imagers. It should be pointed out that phases of the tidal wave perturbations are different in Figure 3(c) and (d), with temperature minimum at midnight in (c) and at 1800LT in (d). This is due to the presence of relatively large non-migrating tides (especially westward diurnal wave 2 component in this case).

The amplitude and phase changes of the planetary wave 1 between day 260 and day 290 at 62.5°N and 42.5°N are plotted in Figure 4. There are large variations in the planetary wave amplitude, but the general trend of an increase in wave 1 activity is evident. At 62.5°N near where the wave amplitude peaks, the phase of the wave is relatively stable before day 274 and af-

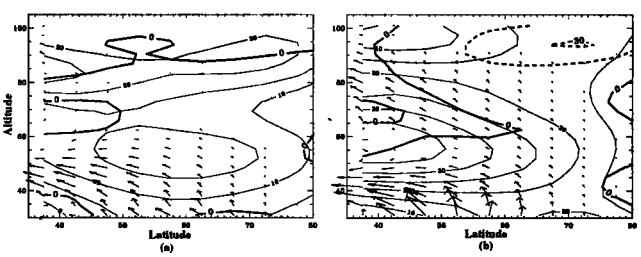

Figure 2. EP flux on day (a)260 and (b)285. The arrows represent direction and magnitude of EP flux and the length scale is the same for both plots. The thin contour lines are the zonal mean wind values (contour interval: 5 m s^{-1}), and the thick contour lines are EP forcing values (contour interval: 15 m $s^{-1}day^{-1}$). Solid contour lines are for eastward direction.

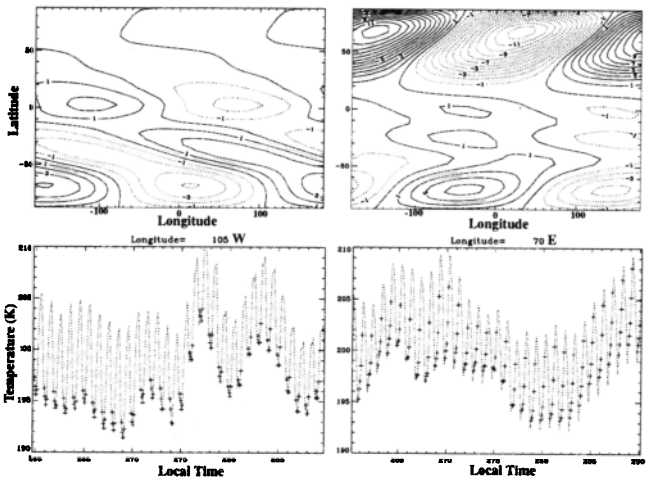

Figure 3. Stationary planetary wave 1 temperature perturbations on day (a)260 and (b)285 at ~87 km, and temperature changes above 2 longitudinal locations at 42.5°N and 87 km from the model: (c)105°W and (d)70°E. The dotted lines are the time series between day 260 and 290, and crosses are at local nights (2100LT-0300LT in (c) and 2000LT-0400LT in (d)) with 2 hours intervals.

ter day 280, indicating the wave is stationary. Between these two days, however, the phase shifts westward by almost 180°. At 42.5°N, there is a similar westward shift of about 220°. The phase shift is related to the phase shift of the NCEP forcing at 10 mb and the associated transience.

The wave 1 growth and phase transience may provide a plausible explanation to the observed large temperature variation around fall equinox (Taylor et al., 2001), where it is shown that the nightly averaged temperature at 87 km altitude increases by about 25 K between day 270 and day 280 above Ft. Collins (41°N, 105°W). As shown by Taylor et al. (2001), the trend of this temperature variation is similar to the variations shown in Figure 3(c), though the observed changes are about 3 times larger than the model results. In the model, the temperature variations between day 270 and 280 correspond to the wave transience. As shown in Figure 4(c) and (d), the amplitude of the wave 1 temperature perturbation increased and its phase shifts westward between day 274 and day 277. On day 274 the phase of the wave 1 temperature perturbation was about 0°, so Ft. Collins was observing the cold sector of the wave. On day 277 the phase of this wave shifted to about 105°W and Ft. Collins was now observing the crest of the warm sector of the wave. This amplitude and phase change of the wave 1 caused a net temperature increase of about 6 K. Detailed analysis of the model results shows that there was also an associated phase change in the wave 2 component which caused a temperature increase of about 2 K. The phase change also led to the temperature decreasing during the same period of time at longitude 70°E. The zonal mean temperature, on the other hand, only increased by about 1 K. The fact that the observed temperature changes are larger than the model results may indicate that the planetary wave temperature perturbations are underestimated in the model. This is confirmed by comparing the temperature amplitude from the model with that from the NCEP at 1 mb and 60°N. They are in reasonable agreement before day 274, but the difference increases rapidly afterward with the NCEP amplitude more than twice as large after day 276.

The wave 1 growth also shows up in the zonal wind perturbations. Figure 5 shows the horizontal and vertical structures of the wave 1 zonal wind perturbations on days 260 and 285. Both wave amplitude and phase structures undergo considerable change during the fall equinox. The peak value of the wave amplitudes at ~96 km and 30°N increases from ~5 ms^{-1} to ~15 ms^{-1}, and the tilting of the phase lines changes from eastward-equatorward to westward-equatorward. On day 260, wave 1 zonal wind perturbation peaks in the southern hemisphere and penetrates to the northern hemisphere with a secondary peak at the equator. This agrees with the global stationary wave 1 structures calculated by Medvedev et al. (1991). On day 285, the wave 1 peak shifts to the northern hemisphere and the structure there is similar to the stationary planetary wave under winter conditions as seen in the WINDII wind data (Wang et al., 2000). Therefore the rapid transition of the planetary wave around equinox is also reflected in its zonal wind component.

As shown in Figure 5(c) and (d), the vertical phase lines of the wave have a characteristic westward tilting on day 285 but not on day 260, and the former indicates a forced planetary wave 1 with large vertical wavelength (>100 km). The phase lines on day 285 also show a distortion above 85 km. This is due to the superposition

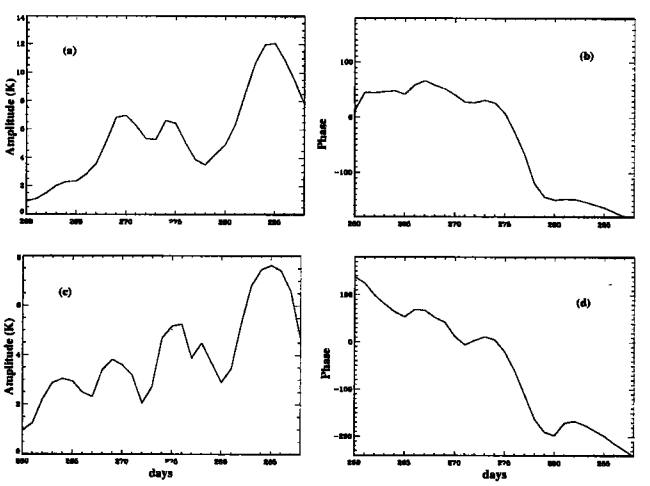

Figure 4. The amplitude and phase changes of stationary planetary wave 1 temperature perturbations at 62.5°N and 42.5°N between day 260 and 290. (a)amplitude, 62.5°N; (b)phase, 62.5°N; (c)amplitude, 42.5°N; (b)phase, 42.5°N. Some phases are shifted 360° for better viewing.

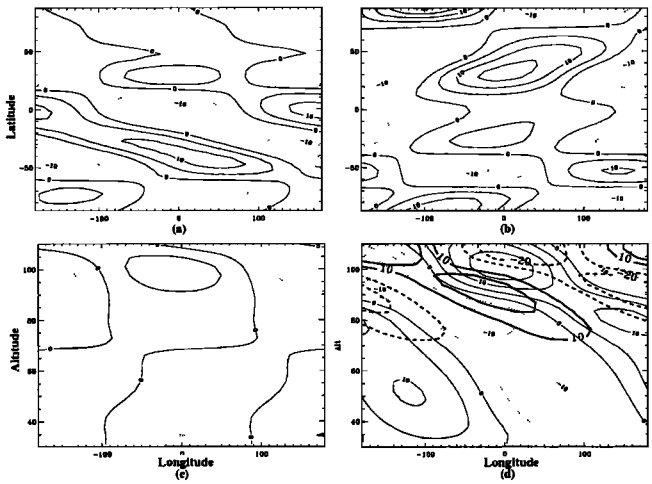

Figure 5. Stationary planetary wave 1 zonal wind perturbations at ~96 km on day (a)260 and (b)285; and at 32.5°N on day (c)260 and (d)285. The thick contour lines in (d) are the gravity wave forcing values (m $s^{-1}day^{-1}$) with solid lines for eastward forcing.

of an in situ forced planetary wave 1 by breaking gravity waves on the primary planetary wave (Smith, 1996; Meyer, 1999). The thick contour lines are the corresponding stationary wave 1 component of the gravity wave forcing with a peak value of ~25 $ms^{-1}day^{-1}$ at 90 km. The peak forcing is along the zero wind perturbation line of the planetary wave and in the area where the slopes of the phase lines are changing, which clearly demonstrates the interactions of gravity waves and the planetary wave.

4. Conclusion

The model results show that planetary wave 1 grows rapidly in the mesosphere around the northern hemisphere fall equinox and the peak of the planetary wave activity shifts from the southern hemisphere to the northern hemisphere. The surge of the planetary wave causes an easterly mean flow acceleration in the mid/high latitude upper mesosphere. The simulated planetary wave structure, in-situ planetary wave forcing due to gravity wave breaking, and the rapid transition around equinox compare favorably with previous climatological and theoretical studies. Wave transience associated with the transition can lead to fast changes in both phase and amplitude of the planetary waves. These changes may cause large variability in local temperature measurements at mid/high latitudes. This provides a qualitative explanation for the large temperature variations observed around the fall equinox by Taylor et al. (2001). The modeled temperature variations, however, are smaller than the measured quantities, which suggests that the planetary wave temperature perturbations or their transience at mid-latitudes might be underestimated by the model.

Acknowledgments. The authors would like to thank C. K. Meyer for helpful discussions and comments. Efforts by HLL and RGR were supported in part by NASA grant S-97239-E to NCAR. The CEDAR mesospheric temperature measurements were supported by NSF grants ATM-9403474 and ATM-9612810. The National Center for Atmospheric Research is sponsored by NSF.

References

Barnett, J. J., and K. Labitzke, Climatological distribution of planetary waves in the middle atmosphere, *Adv. Space Res., 10,* (12)63-(12)91, 1990.

Charney, J. G., and P. G. Drazin, Propagation of planetary scale disturbances from the lower atmosphere into the upper atmosphere, *J. Geophys. Res., 66,* 83-109, 1961.

Medvedev, A. S., A. I. Pogorel'tsev, and S. A. Sukhanova, Modeling the global structure of stationary planetary waves and their penetration across the equator, *Izv. Russ. Acad. Sci. USSR Atmos. Oceanic Phys.* Engl. Transl., *31,* 574-581, 1991.

Meyer, C. K., Gravity wave interactions with mesospheric planetary waves: A mechanism for penetration into the thermosphere-ionosphere system, *J. Geophys. Res., 104,* 28,181-28,196, 1999.

Randel, W. J., Global atmospheric circulation statistics, 1000-1 mb, *NCAR/TN-366+STR,* NCAR, Boulder, Colo., 1992.

Roble, R. G., and E. C. Ridley, A thermosphere-ionosphere-mesosphere-electrodynamics general circulation model (TIME-GCM): equinox solar cycle minimum simulations (30-500km), *Geophys. Res. Lett., 21,* 417-420, 1994.

Shepherd, G. G., J. Stegman, P. Espy, C. McLandress, G. Thuillier, and R. H. Wiens, Springtime transition in lower thermospheric atomic oxygen, *J. Geophys. Res., 104,* 213-223, 1999.

Smith, A. K., Longitudinal variations in mesospheric winds: Evidence for gravity wave filtering by planetary waves, *J. Atmos. Sci., 53,* 1156-1173, 1996.

Taylor, M. J., W. R. Pendleton, Jr., L. C. Gardner, H.-L. Liu, R. G. Roble, C. Y. She, and V. Vasoli, Large amplitude perturbations in mesospheric OH Meinel temperatures around the autumnal equinox transition period, *Geophys. Res. Lett., this issue,* 2001.

Walterscheid, R. L., G. G. Sivjee, and R. G. Roble, Mesospheric and lower thermospheric manifestations of a stratospheric warming event over Eureka, Canada (80°N), *Geophys. Res. Lett., 27,* 2897-2900, 2000.

Wang, D. Y., W. E. Ward, G. G. Shepherd, and D.-L. Wu, Stationary planetary waves inferred from WINDII wind data taken within altitudes 90-120 km during 1991-1996, *J. Atmos. Sci., 57,* 1906-1918, 2000.

H.-L. Liu and R. G. Roble, NCAR High Altitude Observatory, PO Box 3000, Boulder, CO 80307-3000. (e-mail: liuh@ucar.edu; roble@ucar.edu)

M. J. Taylor and W. R. Pendleton, Jr., Space Dynamics Laboratory & Department of Physics, Utah State University, Logan, UT 84322-4145. (e-mail: mtaylor@cc.usu.edu)

(Received November 24, 2000; accepted February 1, 2001.)